Review to establish characteristics of dust particles close to the Lunar Surface

Vera Assis Fernandes[1,2] and Peter Wurz[1]

[1]Physics Insitute, University of Bern

[2]Museum für Naturkunde-Berlin, Leibniz-Institut für Evolutions- und Biodiversitätsforschung an der Humboldt-Universität zu Berlin

"While the surface is the upper boundary of the lunar crust, it is the lower boundary layer of the tenuous atmosphere and constitutes both a source and a sink for atmospheric gases."
Lucey et al. (2006)

30.06.2011 version 1.0

Table of Contents

1 Introduction

The lunar surface is the point of interaction between the space environment which triggers changes in the physical properties of the materials, and thus a natural laboratory for the study of processes on the surface or airless bodies. Lucey et al. (2006, and references therein).

Lunar regolith (soil) is on the top of the lunar surface and completely covers the underlying bedrock. The only exception may be the steep slopes where the material slides down. This layer results from the continuous bombardment of the airless lunar surface by small and large meteoroids as well as due to the continuous and steady bombardment of the lunar surface by charged atomic particles derived from the Sun and other stars.

The lunar regolith is a layer or mantle of fragmental and unconsolidated rock material that can be residual or transported, and nearly everywhere forms the surface of land and overlies or covers bedrock (Bates & Jackson, 1980). It is a somewhat cohesive, dark to light grey, very-fine, loose, clastic material derived mainly from the mechanical comminution of lunar rocks. All we know from lunar samples is virtually from regolith as no rock from the Apollo or Luna missions was acquired from the bedrock. The regolith thickness is on average 10–20 meters (McKay et al., 1974), and on the maria regions only a few meters (Langevin and Arnold, 1977; Taylor, 1982) as represented in Figure 1. The highland regions are typically covered by a regolith layer thicker than in the mare regions. In the highlands the regolith overlies a mega-regolith that is crudely estimated to be 1 to 3 km thick.

The lunar soil can be found as unconsolidated material forming a powdery layer covering nearly all of the lunar surface, and also as part of rocks, breccias, composed of consolidated material derived from the different regolith components. The two main types of breccias are the regolith breccias and polymict breccias. The latter are consolidated rocks that contain rock, mineral, and glass fragments in a glassy matrix (agglutinates).

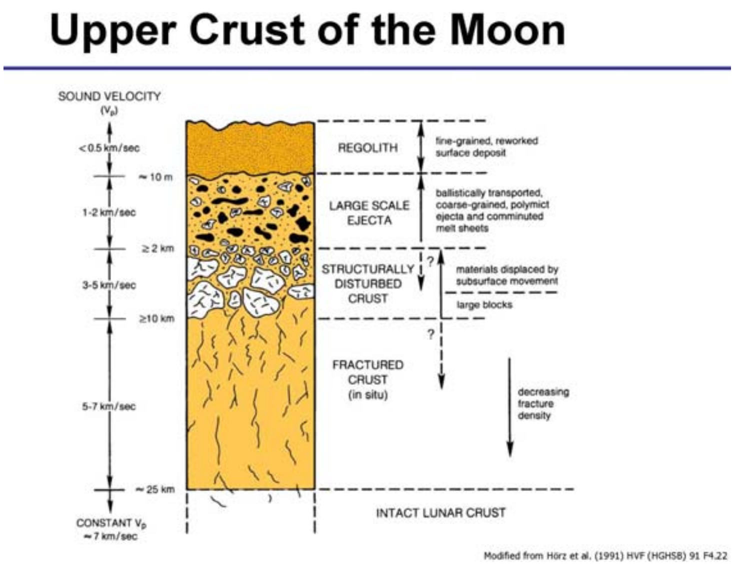

Figure 1: Schematic representation of the lunar upper crust (modified by Kring after Hörz et al., 1991)

The lunar soil is the product of continuous bombardment of the airless lunar surface by micro-meteoritic impact at speeds >10 km/s. This process both comminutes the soil and produces agglutinates. Another important agent for the formation of the lunar regolith is bombardment by the solar wind, which is responsible for the implantation of solar wind gases (^{4}He, ^{20}Ne, ^{36}Ar, ^{84}Kr, ^{132}Xe), spallation nuclides (^{38}Ar, ^{36}Ar) and impacting high-energy particles sputtering which causes the erosion and vaporization of different nuclides.

2 Physical properties of lunar regolith

2.1 Grain size

The Apollo samples were typically subdivided into material for visual estimates at the Lunar Receiving Laboratory and another was sieved into discrete ranges of particle sizes (Table 1). The grouping within the grains for visual inspection was: 0.5–1 mm, 1–2 mm, 2–4mm and 4–10 mm. Soils particles are dominantly < 1 mm in size. Grain mounts were prepared for to sieve finer material for petrologic analyses. The mean grain size ranges from 40 µm to 800 µm, but mostly are 60–80 µm. Some igneous rocks found as clast in the regolith are < 250 µm (Table 1).

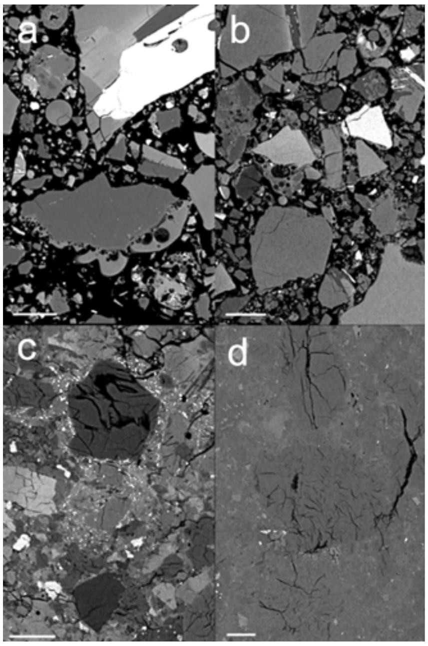

Figure 2: SEM BSE images of lunar regolith breccia samples: a) 79035; b) 10068; c) 15505; and d) QUE 93069 (as a highland breccia, this sample is largely plagioclase and therefore displays little contrast in backscatter). Note the decreasing porosity from (a) to (d). All scale bars are 20 µm (Noble et al., 2010)

Table 1: List of weight distribution versus grain size for sieved soils acquired by Apollo 11, 14, 15, 16 and 17.

Weight distribution (%) per soil						
	< 1mm	1–2 mm	2–4 mm	4–10 mm	> 10 mm	Sample mass (g)
Soil						
10002	89	3.1	2.3	1.6	3.9	476.3
14003	88	3.9	3.0	3.1	2.1	1077.8
14163	87	5.6	3.8	3.8	0	5126.3
15220	95	0.8	1.9	2.3	0	305.2
15270	95	2.5	1.6	0.5	0	837.1
15400	14	0.8	1.0	1.3	83	618.3
62280	78	7.8	4.7	5.1	4.3	279.6
64500	82	4.7	4.0	4.0	5.2	603.6
68500	86	6.3	4.2	2.9	0.2	602.6
70180	25	0.7	0.5	0.3	74	633.1
71500	85	3.2	2.5	1.9	7.4	706.6
72140	95	2.2	0.8	1.1	0.6	237.1
72500	93	3.3	1.8	1.1	0.4	735.3
73240	78	6.0	5.9	9.1	0.7	245.9
78220	96	2.2	1.1	0.6	0	236.5
78500	81	2.4	1.8	2.2	12	884.7

2.2 Soil particles shape

Soil particles are typically irregular and elongated, see Table 2 for characterising parameters.

Table 2: Lunar regolith average shape based on different parameters for particles of 40 to 130 µm

Median particle size 40 to 130 µm		
Avg. particle size	70 µm	~10–20% is finer than 20 µm
Avg. elongation	1.35	somewhat elongated
Avg. aspect ratio	0.55	slightly to medium elongated
Avg. roundness	0.22	subangular to angular
Avg. volume coefficient	0.3	elongated
Avg. specific surface area	0.5 m^2/g	irregular, re-entrant

2.3 Soil-Specific Surface Area

Clays have higher Soil-specific Surface Area (SSA) than lunar soils because of (a) their small size and (b) platy morphology. For a spherical particle, the specific surface area (SSA) is inversely proportional to the diameter, and is given by

$$SSA = \frac{6}{dG\rho_w} \quad (\mathrm{m}^2/\mathrm{g})$$

where d is the diameter of the sphere in micrometers; G is the specific gravity; and ρ_w is the mass density of water, ρ_w = 1 g/cm^3.

Table 3: Comparison of Specific Surface Area of terrestrial clast and lunar soil particles (Carrier et al., 1991)

Surface area of a particle divided by its mass	
Particle Type	Specific Surface Area (m^2/g)
Terrestrial Clays	
Kaolinite	10 – 20
Illite	65 –100
Montmorillonite	50 – 800
Lunar Soil Range	0.02 – 0.78
Lunar Soil Average	0.5

The terrestrial clay minerals have much higher SSA values, due to their very small size and platy shape. Several SSA measurements were conducted on the sub-millimeter lunar soil fraction (Table 3) by means of nitrogen gas adsorption. The SSA values range from 0.02 to 0.78 m^2/g, with a typical value of 0.5 m^2/g, which corresponds to an equivalent spherical diameter of 3.9 µm. Thus, the SSA of lunar soil is much less than that of terrestrial clay minerals, and yet it is significantly larger than can be accounted for by small particle size alone. Instead, the relatively large SSA of lunar soils is indicative of the extremely irregular, re-entrant particle shapes.

2.4 Specific Gravity

Specific Gravity (SG) is the ratio of the density of a substance to the density of a reference substance. SG has been measured for Apollo 11, 12, 14, 15, and 17 soils. The reference substances used with the pycnometry for the case of the lunar soils were nitrogen, helium, water, air, and suspension in a density gradient.

The average specific gravity of a given lunar soil is related to the relative proportions of different particle types; i.e., basalts, mineral fragments, breccias, agglutinates, and glasses. However, the interpretation of the specific gravity is complicated by the porosity of the particles. As illustrated in Figure 3, the porosity may be divided *into three categories (*Figure 3*):*

(1) intergranular porosity, or the volume of space between individual particles

(2) intragranular porosity, or the volume of re-entrant surfaces on the exterior of the particles

(3) *subgranular* porosity, or the volume of enclosed voids within the interior of particles

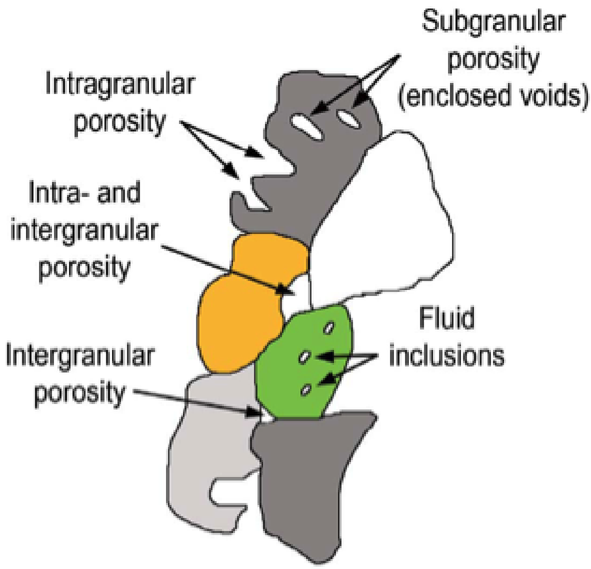

Figure 3: Modified by Kring after Carrier et al. (1991)

Table 4: Summary of Specific gravity determined for different lunar soils and rock fragments (Carrier et al., 1991, and references therein).

Sample Number	Sample Weight (grams)	Specific Gravity, G	Test Technique	References
10004 and 10005	49.1	3.1*	Nitrogen pycnometry	*Costes et al.* (1970a)
10020,44	5.94	3.25†	Water pycnometry	*Horai and Winkler* (1980)
10065,23	4.48	3.12‡	Water pycnometry	*Horai and Winkler* (1980)
10084	1.5	3.01	Suspension in density gradient	*Duke et al.* (1970a)
Apollo 12 (unnumbered)	56.9	3.1*	Air pycnometry	*Carrier* (1970)
12002,85	2.32	2.31‡	Water pycnometry	*Horai and Winkler* (1975)
12029,8	1.10	2.9	Nitrogen pycnometry	R. F. Scott (personal communication, 1988)
12057,72		2.9	Unknown	*Heywood* (1971)
14163,111	0.65	2.9 ± 0.1	Helium pycnometry	*Cadenhead et al.* (1972)
14163,148	0.97	2.90 ± 0.05	Water pycnometry	*Carrier et al.* (1973a, b)
14259,3	1.26	2.93 ± 0.05	Water pycnometry	*Carrier et al.* (1973a, b)
14321,74		3.2 ± 0.1‡	Helium pycnometry	*Cadenhead et al.* (1972)
14321,156		3.2 ± 0.1‡	Helium pycnometry	*Cadenhead et al.* (1972)
15015,29		3.0 ± 0.1‡	Helium pycnometry	*Cadenhead et al.* (1974); *Cadenhead and Stetter* (1975)
15101,68		3.1 ± 0.1	Helium pycnometry	*Cadenhead and Jones* (1972)
15601,82	0.96	3.24 ± 0.05	Water pycnometry	*Carrier et al.* (1973a, b)
70017,77	2.55	3.51†	Water pycnometry	*Horai and Winkler* (1976)
70215,18	4.84	3.44†	Water pycnometry	*Horai and Winkler* (1976)
72395,14	3.66	3.07‡	Water pycnometry	*Horai and Winkler* (1976)
77035,44	3.68	3.05‡	Water pycnometry	*Horai and Winkler* (1976)
Recommended typical specific gravity of lunar soil: 3.1				

* Total soil sample; others were performed on submillimeter fraction.
† Single basalt fragment.
‡ Single breccia fragment.

The bulk lunar soil SG values range from 2.9 to 3.5, and the representative value is 3.1. The SG values for specific types of particles are:

- 1.0 to > 3.32 for agglutinates and glass particles
- > 3.32 for basalt particles
- 2.9 to 3.1 breccia particles
- For comparison, many terrestrial soils have a specific gravity of 2.7; that is, the density of the individual particles is 2.7 g/cm^3, or 2.7 times the density of water (1 g/cm^3).

The enclosed voids in a lunar soil particle with a specific gravity of 1.0 occupy two-thirds of the total volume of the particle (Carrier et al., 1991). Thus, the average specific gravity of the particles would be even greater if there were no enclosed voids. For example, if the lunar soil were ground into a fine powder (in which the resulting particles were smaller than the enclosed voids), these voids would be destroyed, and the specific gravity would be increased (Carrier et al., 1991).

.

The actual subgranular porosity of individual lunar soil particles is only poorly known, and additional measurements of subgranular porosity are needed. The intragranular porosity has a strong effect on the bulk density of the lunar soil, whereas the intergranular porosity affects both the bulk density and the relative density. These relations will be discussed below (Carrier et al., 1991).

.

2.5 Bulk Density and Porosity

2.5.1 Bulk Density

The *in situ* bulk density of lunar soil is a fundamental property. It influences bearing capacity, slope stability, seismic velocity, thermal conductivity, electrical resistivity, and the depth of penetration of ionizing radiation. The *bulk density*, ρ, of soil is defined as the mass of the material contained within a given volume, usually expressed in grams per cubic centimetre. The *porosity*, *n*, is defined as the volume of void space between the particles divided by the total volume. Bulk density, porosity, and specific gravity are interrelated as

$$\rho = SG\, \rho_w\, (1 - n)$$

where, *SG* is the specific gravity (including sub-granular porosity); ρ_w is the density of water (ρ_w = 1 g/cm^3), and *n* is the porosity, expressed as a decimal (combining both inter- and intragranular porosity).

The representative range for the bulk density for an intercrater area is from 1.45 to 1.79 g/cm^3, dependent on depth. Estimates for *in situ* bulk density of different lunar soils are summarised in Table 5. The bulk density was determined using different approaches listed below:

(1) remote sensing techniques (passive VIS, IR, and microwave emissivity and active radar reflectivity) - 0.3–0.4 g/cm^3;
(2) in situ robotic measurements by Surveyor 1, 3, and 7; Luna 13; Luna 17/Lunokhod 1; Luna 21/Lunokhod - 0.8 to 1.7 g/cm^3.
(3) Correlation lunar observations (astronaut bootprints, vehicle tracks, boulder tracks) with those of simulated lunar soil, and also perform experiments to measure the penetration resistance - 1.34 to 1.92 g/cm^3.

(4) Laboratory measurements on cores (i.e., Apollo 11, 12, 14, 15, 16, and 17; Luna 16, 20, and 24; Fig. 4) 0.75 to 2.29 g/cm^3.

Table 5: Estimates for in-situ bulk density of different lunar soils (Carrier et al., 1991)

Source	Bulk Density, (g/cm^3)	References
Remote Sensing	0.3	*Jaffe* (1964, 1965)
	0.4	*Halajian* (1964)
Robotic Measurements on Surface		
Surveyor 1	1.5	*Christensen et al.* (1967)
Luna 13	0.8	*Cherkasov et al.* (1968)
Surveyor 1, 3, and 7	1.5	*Scott and Roberson* (1967, 1968a,b); *Scott* (1968)
Surveyor	1.1 at surface; 1.6 at 5 cm	*Jaffe* (1969)
Lunokhod 1/Luna 16	1.5–1.7	*Leonovich et al.* (1971, 1972)
Surveyor 3	1.7	*Jaffe* (1973)
Lunokhod 1 and 2/Luna 16 and 20	1.5	*Leonovich et al.* (1974a, 1975)
Correlations with Simulated Lunar Soil		
Astronaut Bootprints		
Intercrater area	1.45 - 1.59	*Mitchell et al.* (1974)
Crater rims (depth 0-15 cm)	1.34 - 1.57	*Mitchell et al.* (1974)
Vehicle Tracks		
MET and LRV (depth 0-15 cm)	1.40 - 1.56	*Mitchell et al.* (1974)
Boulder Tracks (depth 0-300 to 400 cm)	1.38 - 1.68	*Mitchell et al.* (1974)
Penetration Resistance		
Apollo 11	< 1.81 - 1.92	*Costes et al.* (1971)
Apollo 12	< 1.80 - 1.84	*Costes et al.* (1971)
Lunokhod 1 and Apollo 14-16 (depth 0-60 cm)	1.58 - 1.76	*Mitchell et al.* (1974)
Returned Core Samples		
Apollo 11	1.54 - 1.75	*Costes and Mitchell* (1970)
	0.75 ->1.75	*Scott et al.* (1971)
Apollo 12	1.6 - 2.0	*Scott et al.* (1971)
	1.55 - 1.90	*Houston and Mitchell* (1971)
	1.7 - 1.9	*Carrier et al.* (1971)
Luna 16	1.2	*Vinogradov* (1971)
Apollo 14	1.45 - 1.6	*Carrier et al.* (1972a)
Apollo 15		
Core Tubes	1.36 - 1.85	*Carrier et al.* (1972a); *Mitchell et al.* (1972a)
Drill Cores	1.62 - 1.93	*Carrier* (1974); *Mitchell et al.* (1972a)
Luna 20	1.1 - 1.8	*Vinogradov* (1972)
Apollo 16		
Core Tubes	1.40 - 1.80	*Mitchell et al.* (1972b)
Drill Cores	1.47 - 1.75	*Carrier* (1974)
Apollo 17		
Core Tubes	1.57 - 2.29	*Mitchell et al.* (1973a)
Drill Core	1.74 - 1.99	*Carrier* (1974)
Luna 24	1.6 - 2.1	*Florensky et al.* (1977); *Barsukov* (1977)
Best Estimates: Typical Average Values (Intercrater Areas)		*Mitchell et al.* (1974)
Depth Range (cm)		
0 - 15	1.45 - 1.55	
0 - 30	1.53 - 1.63	
30 - 60	1.69 - 1.79	
0 - 60	1.61 - 1.71	

Best average estimates for bulk density of lunar soil as estimated by Mitchel et al., (1974). The values reported in Table 6 take into account all the measurements, approximations, analyses, qualifications, and uncertainties:

Table 6: Best estimates of bulk density vs. depth range.

Average Bulk Density (g/cm³)	Depth Range (cm)
1.50 ± 0.05	0 - 15
1.58 ± 0.05	0 - 30
1.74 ± 0.05	30 - 60
1.66 ± 0.05	0 - 60

The typical average bulk density of the lunar soil is 1.50 ± 0.05 g/cm^3 for the top 15 cm, and 1.66 ± 0.05 g/cm^3 for the top 60 cm. However, the fine details of how the density (Carrier et al., 1991) varies with depth, particularly very near the surface, are not really known. With respect to the dust above the surface (in the atmosphere) one can assume that its origin is mostly within the top surface layer.

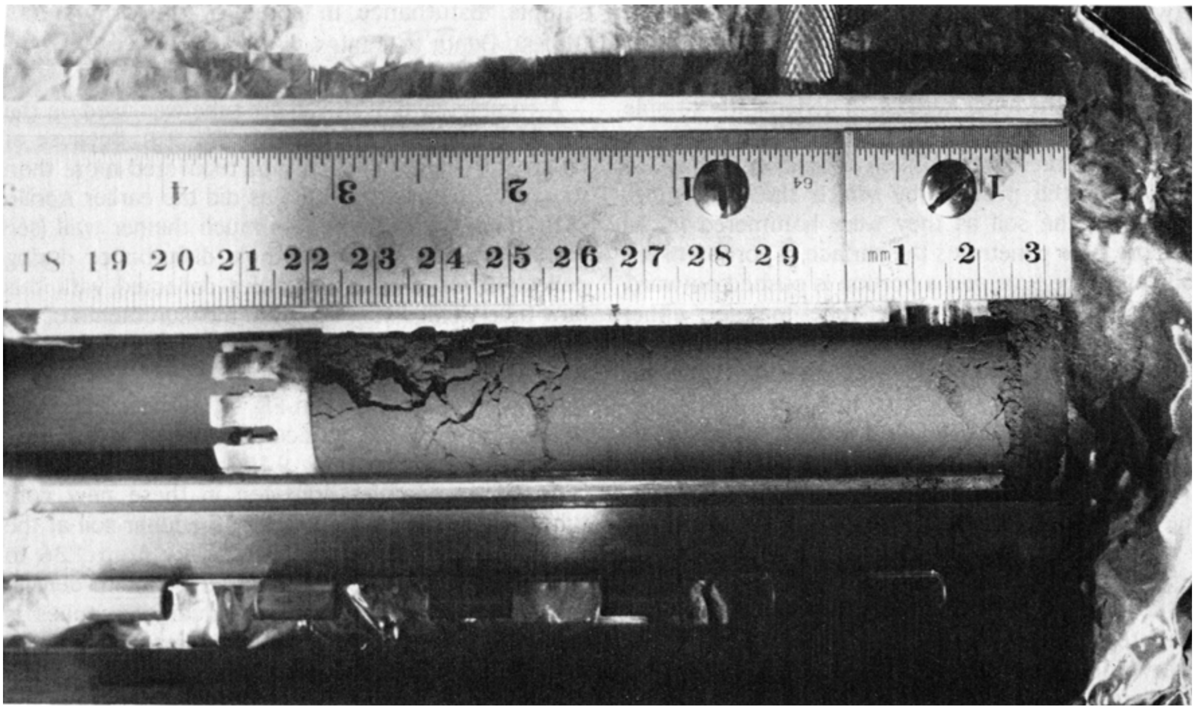

Figure 4 Photograph of Apollo 11 core tube sample 10005 (S/N 2007), immediately after opening of the tube in the Lunar Receiving Laboratory at the NASA Johnson Space Center in 1969 (NASA Photo S-69-45048.).

2.5.2 Porosity

The *in situ* porosity (n) of lunar soil is calculated by combining the best estimates of bulk density (Table 6) and specific gravity (Table 4), the results are presented in Table 7 below:

Table 7: Best estimates of lunar soil in situ porosity (inter- and intragranular porosity combined).

Depth Range (cm)	Average Porosity, n (%)	Average Void Ratio, e
0 - 15	52 ± 2	1.07 ± 0.07
0 - 30	49 ± 2	0.96 ± 0.07
30 - 60	44 ± 2	0.78 ± 0.07
0 - 60	46 ± 2	0.87 ± 0.07

2.5.3 Relative Density

Another way to perceive density is associated with the relative arrangement of the soil particles. A soil consisting of uniform spheres could be arranged in face-centred cubic packing. Such a packing is the loosest possible stable arrangement. Under these conditions, the porosity of the soil would be 47.6% and the void ratio would be 0.92. If the specific gravity of the spheres were 3.1, the bulk density of the soil would be 1.61 g/cm^3. On the other hand, the spheres could be arranged in hexagonal close packing. In this case the soil particles are more densely packed without deforming or breaking the particles, and require 30% less volume. The porosity would now be 26.0%, the void ratio would be 0.35, and the bulk density would be 2.30 g/cm^3.

2.6 Compressability

Compressibility describes the volume change, or densification, that occurs when a confining stress is applied to soil. At low stress or low initial density, compression of the soil results from particle slippage and reorientation. At high stress or high initial density, particle deformation and breakage at the points of contact also occur. A summary of compressibility parameters is presented in Table 8 and discussed in the following sections.

Compression index. The *compression index, Cc,* is defined as the decrease in void ratio that occurs when the stress is increased by an order of magnitude

$$Cc = \frac{\Delta e}{\Delta \log \sigma_v} = -\frac{de}{d \log \sigma_v}$$

where Δe is the change in void ratio (negative) and $\Delta \log \sigma_v$ is the change in logarithm of applied vertical stress.

Table 8: Compressibility parameters of lunar soil.

Parameter	Range	Recommended Typical Value
Compression Index, C_c		
Loose		0.3
Dense	0.01 – 0.11	0.05
Recompression Index, C_r	0.000 – 0.013	0.003
Maximum Past Pressure		Unknown
Coefficient of Lateral Stress, K_o		
Normally consolidated	0.4 – 0.5	0.45
Over-consolidated		Unknown
Recompacted		0.7

2.7 Electrostatic Charging and Dust Migration

A large number of observations of *lunar transient events,* especially unexplained glows and obscurations, have been noted over two centuries of ground-based observations, continuing up to the present (*Cameron,* 1974, 1978). These changes in lunar brightness may have rise times of < 1 sec to 5 sec and range in colour from reddish to bluish. One of the plausible explanations for a possible mechanism are electrical phenomena in the lunar surface layers (Carrier et al., 1991). The large electrical conductivity change with visible and UV irradiation, combined with the very low electrical conductivity and dielectric losses of lunar materials, can produce an extremely efficient electrostatic charging mechanism between opposite sides of the lunar terminator. Across this moving boundary, charging of lunar soil particles could be sufficient to levitate them above the surface, producing a “dust storm” of particles that would follow the solar terminator around the Moon (Carrier et al., 1991).

2.7.1 Electrical Conductivity

Electrical conductivity is a measure of how easily electrical current flows through a material, i.e., how easily electrical charge may be transported through it. High electrical conductivity means that the material easily carries electrical current and does not readily remain electrically charged. Low electrical conductivity means that the material does not easily transport charge and tends to remain electrically charged. The electrical conductivity of lunar materials at low frequencies (below 1 Hz) is essentially the same as of DC (0 Hz) conductivity, and is extremely low (Table 9), and is dominantly controlled by temperature.

A soil from the Apollo 15 site (sample 15301,38) exhibits a temperature dependence of conductivity (Fig. 5) of the form

$$DCconductivity = 6\times 10^{-18} e^{0.0237T} mho/m$$

where *T* is the absolute temperature (Kelvin) (Olhoeft et al., 1974). This type of temperature dependence is characteristic of amorphous materials and is typical of the heavily radiation-damaged lunar soil particles. *The low frequency electrical conductivity of lunar rocks is typical of terrestrial silicates in the total absence of water*.

Table 9: DC electrical conductivity of lunar rocks.

Lunar Sample	σ_0* mho/m	E_0† eV	σ_1 mho/m	E_1 eV
10048	3.5	0.896	2.66×10^{-3}	0.559
12002,85	13	1.09	1.8×10^{-4}	0.48
15058	134	1.374	2.78×10^{-3}	0.593
15418	137	1.509	9.84×10^{-2}	0.971
15555	36.8	1.040	1.27×10^{-2}	0.604
68415	1.27×10^{8}	2.640	0	0
68815	14.2	1.366	0	0

* Conductivity.
† Activation energy.

Data for sample 12002 are from *Olhoeft et al.* (1973); the rest are from *Schwerer et al.* (1974).

Fehler! Verweisquelle konnte nicht gefunden werden. shows the electrical conductivity of lunar samples. DC conductivity (vertical axis) is plotted as a function of inverse temperature in kelvins (bottom horizontal axis) and temperature (top horizontal axis), using the equations given in the text. In general, conductivity increases with increasing temperature for both lunar soil and rock samples. Dashed curves (from *Schwereret al.,* 1974) are for samples 10048, 15058, 15418, 15555, 68415, and 68815. Solid curves (*Olhoeft et al.,*1973) give data for two soil samples (12002,85 and 15301,38) and one rock (65015,6).

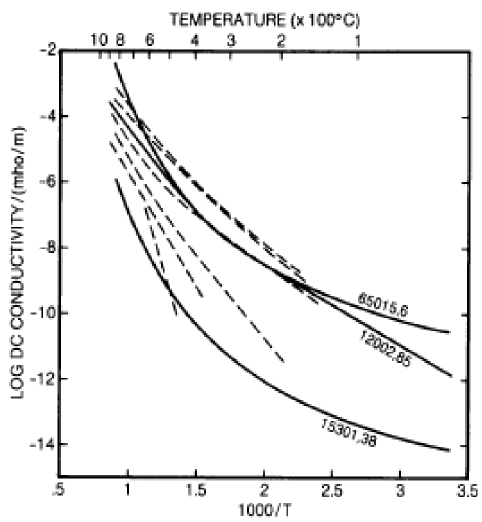

Figure 5: Electrical conductivity of lunar samples.

The temperature dependence of one Apollo 16 rock (sample 65015,6) (Olhoeft et al., 1973) was similar in form to that of soil

$$DCconductivity = 3 \times 10^{-14} e^{0.0230T} \quad \text{mho/m}$$

However, the temperature dependence of the electrical conductivity measured on the remaining lunar rocks (**Fehler! Verweisquelle konnte nicht gefunden werden.**) was found to be given by

$$DCconductivity = \sigma_0 e^{-E_0/k_B T} + \sigma_1 e^{-E_1/k_B T} \quad \text{mho/m}$$

where, k_B = Boltzmann's constant = 8.6176 × 10^{-5} eV/K and T is the absolute temperature (Kelvin), and E_0 and E_1 are activation energies (Table 9). Because these lunar materials have very low conductivities, dielectric relaxation effects and displacement currents dominate at very low frequencies. Further details on electrical conductivity of lunar rocks are provided by Olhoeft et al. (1973) and Schwerer et al. (1974).

2.8 Soil Composition

The bulk composition of lunar soils varies from anorthositic to basaltic plus a small amount of meteoritic material (< 2%, Papike et al., 1998), see Figure 6 for an overview of the mineralogical composition. A few examples of typical mineralogical composition (modal mineral fraction in %) of soils from the Apollo missions landing sites are presented in the Tables 10 and 11 below. These two soils, 71061,1 (Table 10) and 64501 (Table 11) represent typical mare and highland derived soils, respectively.

Modal Mineral composition of a typical highland and a mare soil

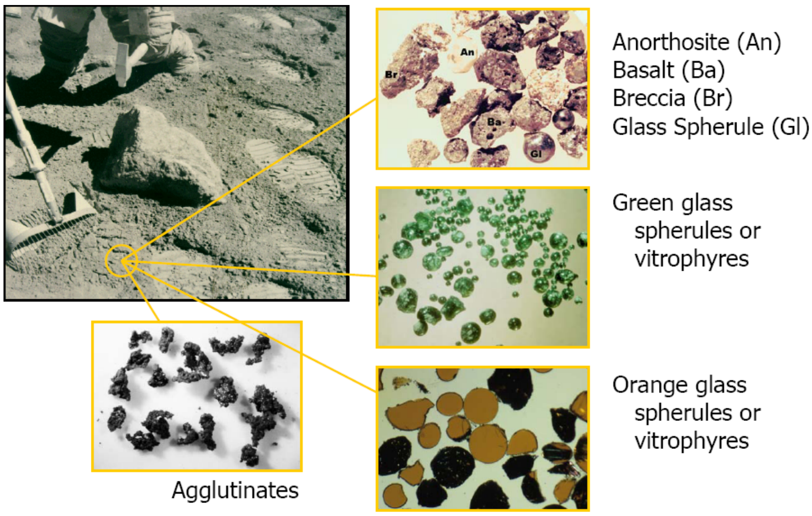

Figure 6: Typical lunar soil and its components (Image by Kring D.)

Table 10: Modal mineral fraction in % for Apollo 17 soil 71061,1 (McKay et al., 1991)

71061,1 (a typical Apollo 17 mare soil)											
	Petrographically Determined Vol%							Visual Estimate %			
particle size (µm)	<20	20-45	45-75	75-90	90-150	150-250	250-500	0.5-1	1-2	2-4	4-10
Agglutinates	17	17	13	17	9	12	10	-	-	-	-
Basalt, equigran.	-	-	9	15	31		-	-	-	-	-
Basalt, variolitic	-	-	1	2	20	3	52	65	100	100	100
Breccia	-	-	2	7	6	8	8	-	-	-	-
Anorthosite	-	-	1	-	<1	1	-	-	-	-	-
Norite	-	-	-	-	-	-	-	-	-	-	-
Gabbro	-	-	-	-	-	-	0.5	5	-	-	-
Plagioclase	-	-	16	7	17	9	9	-	-	-	-
Pyroxene	-	-	21	26	21	17	11	-	-	-	-
Olivine	-	-	-	-	-	1	-	-	-	-	-
Ilmenite	-	-	6	3	5	3	2	-	-	-	-
Glass	-	-	28	22	22	15	8	15	-	-	-
Other	(83)	(83)	2	-	-	1	-	-	-	-	-
Fractional Wt%	18	12	8	3	9	7	7	3	6	7	10

Table 11: Modal mineral fraction in % for Apollo 16 soil 64501.

64501 (a typical Apollo 16 highland soil)											
	Petrographically Determined Vol%							Visual Estimate %			
particle size (µm)	<20	20-45	45-75	75-90	90-150	150-250	250-500	0.5-1	1-2	2-4	4-10
Agglutinates	-	23	26	35	44	27	28	-	-	-	-
Basalt	-	-	-	-	-	-	-	-	-	-	-
Breccia	-	23	22	24	26	33	31	-	-	-	-
Anorthosite	-	-	-	<1	-	<1	6	-	-	-	-
Norite	-	-	-	-	-	-	-	-	-	-	-
Gabbro	-	-	-	-	-	-	-	-	-	-	-
Plagioclase	-	34	43	29	25	34	29	-	-	-	-
Pyroxene	-	7	2	2	<1	1	-	-	-	-	-
Olivine	-	2	<1	1	-	-	-	-	-	-	-
Ilmenite	-	1	-	-	-	-	-	-	-	-	-
Glass	-	9	8	9	5	5	4	-	-	-	-
Other	-	<1	<1	-	-	-	-	-	-	-	-
Fractional Wt%	-	16	10	4	10	8	9	-	-	-	-

2.8.1 Chemical composition on bulk soils from different landing sites (Papike et al., 1998):

The chemical composition of lunar soils reflects their mixing of different components. The soil samples collected by the Apollo missions show the existence of exotic material to the site where they were obtained. For example, despite the fact that the Apollo 11 mission landed in the middle of the mare plain, the soils do not have compositions equivalent to 100% mare basalt: other rock and minerals from the anorthositic highlands, rare KREEP-bearing minerals and even a small meteoritic component are also included. Table 12 shows chemical abundances for soils from Apollo and Luna missions as recalculated by Wurz et al. (2007).

Table 12: Wurz et al. (2007) report Lunar reference suite soils (including Apollo 15 sample 15601) for Highland, KREEP, low-Ti and high-Ti Mare regions. Data were taken from Papike et al. [1982] and are reported in mole-%. Original literature on Luna soil chemistry lacks in reporting values for Si [Laul and Papike, 1981]. Therefore, we assigned average wt-% values of Si to empty Luna Si entries (marked by asterisk). All data are normalized to 100%.

Reference suite Highland soils	**Size fraction**	**Si**	**Ti**	**Al**	**Fe**	**Mg**	**Ca**	**Na**	**K**	**Mn**	**Cr**	**O**	**Total**
64501,122	bulk	16.26	0.10	11.72	1.26	2.62	6.61	0.31	0.05	0.02	0.03	61.03	100
67461,74	bulk	16.09	0.08	12.31	1.26	2.08	6.74	0.30	0.03	0.02	0.02	61.09	100
22001,35	>125 µm	*16.18	0.13	9.95	2.18	5.19	5.43	0.24	0.03	0.03	0.05	60.59	100
72501,15	bulk	16.57	0.39	8.69	2.91	5.47	4.91	0.31	0.08	0.04	0.07	60.57	100
average		16.31	0.17	10.66	1.90	3.84	5.92	0.29	0.05	0.03	0.04	60.82	100
KREEP soils													
12001,599	bulk	17.21	0.79	5.51	5.38	5.80	4.37	0.35	0.12	0.07	0.12	60.29	100
12033,464	bulk	17.47	0.64	6.23	4.80	5.11	4.43	0.48	0.19	0.06	0.11	60.47	100
14163,778	bulk	17.37	0.44	7.70	3.22	5.26	4.49	0.50	0.26	0.04	0.06	60.66	100
average		17.35	0.62	6.48	4.47	5.39	4.43	0.44	0.19	0.06	0.10	60.47	100
low-Ti Mare soils													
12001,599	bulk	17.21	0.79	5.51	5.38	5.80	4.37	0.35	0.12	0.07	0.12	60.29	100
15601	bulk	17.39	0.57	4.64	6.39	6.27	4.09	0.22	0.05	0.08	0.17	60.12	100
21000,5	bulk	*16.80	0.98	6.82	5.15	4.51	4.72	0.27	0.05	0.07	0.09	60.54	100
24999,6	bulk	*17.29	0.29	5.29	6.48	5.55	4.56	0.20	0.01	0.09	0.14	60.09	100

Another fraction of nuclides of potential interest are the solar wind components found reappeared in agglutonitic soil particles (usually magnetic due to the existence of Fe° nanophase).

Table 13 shows the concentrations of solar-wind elements in magnetic agglutinate fractions separated from soil 15601. Moreover, Table 14 shows the surface and volume correlated concentrations of solar-wind elements (in cm^3 STP/g) in agglutinates from same soil.

Agglutinates, which are a large component of the lunar regolith, formed as the result of surface exposure, then will also be exposed to more surface processes, and especially resulting from the bombardment by extra-lunar charged solar wind particles, solar flares, and cosmic rays. Solar-wind ions implant themselves in a thin outer rind of any soil target (e.g., an agglutinate particle), with varying degrees of efficiency; the penetration depth for an element is no more than a few hundred angstroms. Thus, the solar-wind atoms, implanted after the agglutinate formed, can be considered to reside at the surface of the agglutinate. However, older solar-wind particles occur inside agglutinates in the small soil particles contained within the agglutinates. These older soil particles were irradiated by the solar wind for various lengths of time before they were incorporated into the newly formed agglutinates.

Table 13: Concentrations of solar-wind elements (in cm^3 STP/g) in magnetic agglutinate fractions separated from soil 15601.

	Range of grain size [μm]												
									Repurified				
Isotope	20–30	30–40	40–53	53–75	75–106	106–150	150–250	250–1000	10–20	20–30	30–40	40–53	53–75
^{3}He[10^{-5}]	2.02	2.08	1.57	1.10	1.04 0.996	0.845	0.778	0.854 0.663	2.62	2.34	1.90	1.71	1.25
^{4}He[10^{-2}]	5.21	5.28	3.99	2.88	2.64	2.20 2.58	2.01	2.23	6.62 1.60	5.94	4.91	4.33	3.23
^{20}Ne[10^{-5}]	142	149	110	88.9	85.8 83.3	75.5	65.9	76.7 58.0	183	161	136	122	95.9
^{21}Ne[10^{-5}]	0.390	0.417	0.325	0.258	0.262 0.254	0.231	0.209	0.240 0.193	0.491	0.449	0.381	0.344	0.28
^{22}Ne[10^{-5}]	11.4	11.8	8.96	7.19	6.96 6.74	6.07	5.38	6.19 4.61	14.8	13.0	11.0	9.94	7.85
^{36}Ar[10^{-5}]	41.4	38.4	29.4	25.9	21.8 22.7	19.7	17.6	19.3 14.6	52.1	42.0	36.4	31.7	26.3
^{38}Ar[10^{-5}]	7.81	7.22	5.51	4.88	4.16 4.24	3.71	3.32	3.65 2.71	9.87	7.91	6.93	5.97	4.98
^{40}Ar[10^{-5}]	36.2	33.5	26.7	23.1	19.2 20.2	18.7	17.7	16.9 13.1	45.1	35.7	30.5	27.1	23.2
^{84}Kr[10^{-8}]	25.7	22.7	19.5	17.0	13.7 14.8	13.2	12.5	12.2 9.9	35.8	28.7	25.2	22.0	18.7
^{132}Xe[10^{-8}]	4.27	3.36	2.83	2.69	2.01 2.18	2.14	1.90	1.79 1.50	5.29	4.38	3.69	3.34	2.80

The weight of the samples analyzed varied between 0.45 and 2.1 mg. Included are also "repurified" agglutinate separates, samples that were received after three sequential magnetic separations to make sure that no nonmagnetic material was left (*Schultz et al.*, 1977).

Table 14: Surface and volume correlated concentrations of solar-wind elements (in cm^3 STP/g) in agglutinates from soil 15601.

Element	S	V
^{4}He[10^{-4}]	106 ± 13	131 ± 20
^{20}Ne[10^{-4}]	2.46 ± 0.25	5.45 ± 0.40
^{36}Ar[10^{-4}]	0.72 ± 0.06	1.44 ± 0.13
^{84}Kr[10^{-8}]	4.12 ± 022	10.4 ± 0.5
^{132}Xe[10^{-8}]	0.68 ± 0.04	1.52 ± 0.09

S is the concentration in the fraction of 100 diameter. V is the grain size independent volume correlated component. (Uncertainties given correspond to 1 sigma error of the fit.)

3 Dust Fountains and Electrostatic Levitation

"There is much evidence to show that lunar `horizon glow´ and ´streamers´ observed at the terminator are caused by sunlight scattered by dust grains originating from the surface. The dust grains and lunar surface are electrostatically charged by the Moon´s interaction with the local plasma environment and the photoemission of electrons due to solar UV and X-rays. This effect causes the like-charged surface and dust particles to repel each other, and creates a near-surface electric field. Previous models have explained micron-sized dust observed at 10 cm above the surface, by suggesting that charged grains ''levitate'' in the local electric field; however this cannot account for observations of 0.1 μm-scale grains at ~100 km altitude. In order to explain the high-altitude dust observations, we propose a dynamic ''fountain'' model (Figure 7) in which charged dust grains follow ballistic trajectories, subsequent to being accelerated upward through a narrow sheath region by the surface electric field. These dust grains could affect the optical quality of the lunar environment for astronomical observations and interfere with exploration activities" (Stubbs et al., 2006).

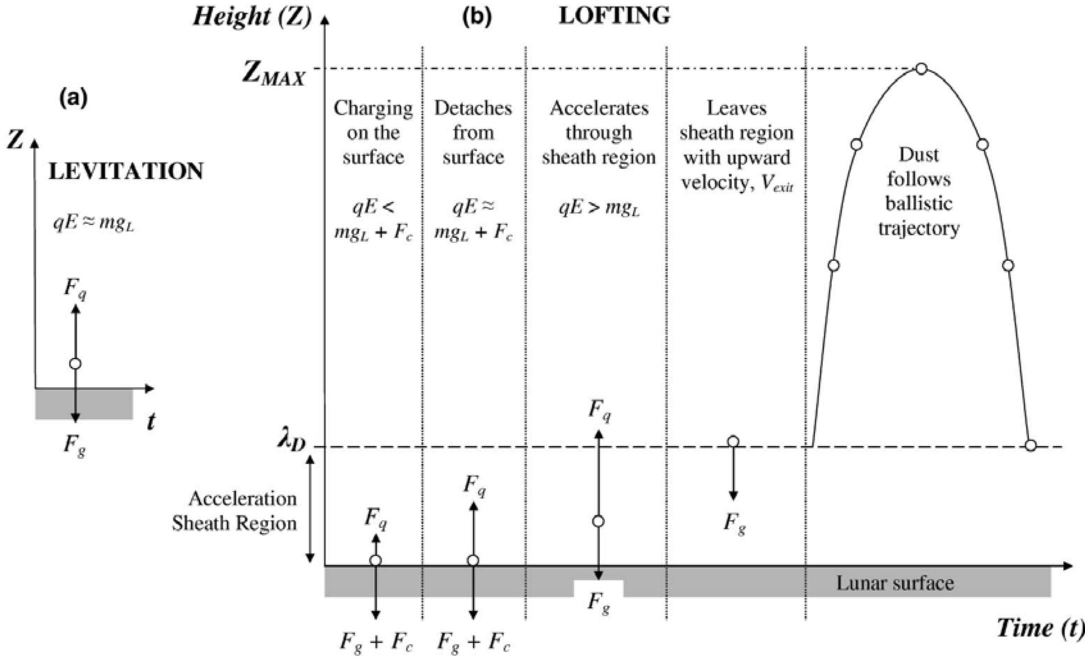

Figure 7: Schematic comparing (a) the static levitation concept, as suggested by Criswell (1973) and others, with (b) the evolution of a dust grain in Stubbs et al., (2006) dynamic fountain model.

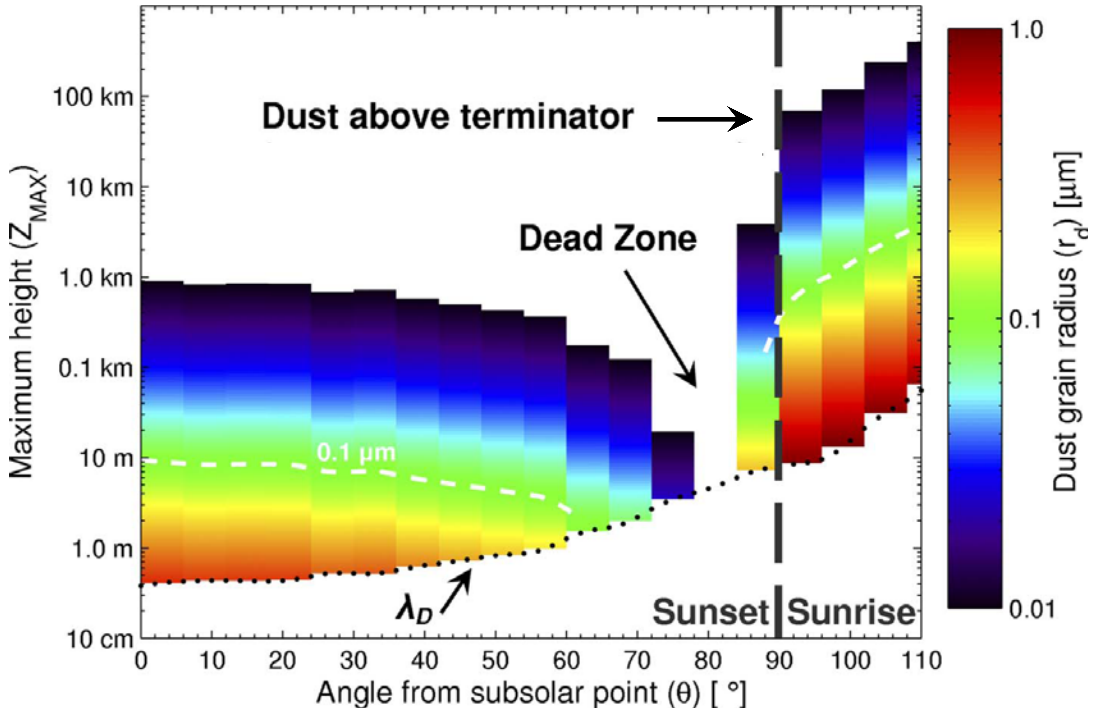

Figure 8: Spectrogram plot showing fountain model predictions for the maximum dust grain height reached (ZMAX) as a function of angle from the subsolar point (h) and dust grain radius (rd). The contour for the predicted altitude reached by 0.1 µm dust grains is indicated by the broken white line. The Debye length (λ_D) is represented by the black dotted line, and marks the extent of the ''Acceleration Sheath Region'' in this model (see Figure 7), from Stubbs et al. (2006).

4 Brief consideration of the impact to Human and technological activities

4.1 *Human Health Concerns*

There are concerns that the dust found on the lunar surface could cause harmful effects on any manned outpost technology and crew members:

- Abrasive nature of the lunar dust particles may rub and wear down surfaces through friction;
- Negative effect on coatings used on gaskets to seal equipment from space, optical lenses that include solar panels and windows as well as wiring;
- Possible damage to an astronaut's lungs, nervous, and cardiovascular systems.

The harmful properties of the lunar dust are not well known. However, based on studies of dust found on Earth, it is expected that exposure to lunar dust will result in greater risks to health both from direct exposure (acute) and if exposure is over time (chronic). This is because lunar dust is more chemically reactive, has larger surface areas, and is composed of sharper jagged edges than Earth dust (Park et al., 2006; Cain, 2010). If the chemical reactive particles are deposited in the lungs, they may cause respiratory disease. Long-term exposure to the dust may cause a more serious respiratory disease similar to silicosis. During lunar exploration, the astronaut's spacesuits will become contaminated with lunar dust. The dust will be released into the atmosphere when the suits are removed. The methods used to mitigate exposure will include providing high air recirculation rates in the airlock, the use of a "Double Shell Spacesuit", the use of dust shields, the use of high grade magnetic separation and the use of solar flux to sinter and melt the regolith (Cain, 2010).

4.2 *Interference with Instrumentation*

Furthermore, Muphy and Vondrak (1993) and Stubbs et al. (2006) have concluded that submicron dust grains could contaminate astronomical observations of infra-red, visible and UV light over the majority of the lunar surface, and not just at the terminator. This is one of many ways in which dust could interfere with science and exploration activities on the Moon; therefore a thorough understanding of lunar dust behaviour is necessary to effectively tackle these problems in the future.

4.3 *Trafficability*

Another issue is trafficability or the capacity of a soil to support a vehicle and to provide sufficient traction for movement. The primary limitations on the trafficability of the lunar soil are speed and slope climbing. The normal cruise speed of the LRV was 6–7 km/hr. This speed was constrained by the irregularity of the cratered surface, coupled with the low lunar gravity. The speed of a future lunar vehicles can be increased only by modifying its dynamic response (e.g., by using larger diameter wheels, an increased wheel base, greater mass, or a softer suspension system), and/or by constructing permanent roads.

5 References:

Bates R. L. and Jackson J. A., eds. (1980) *The Glossary of Geology, 2nd edition.* American Geological Institute, Washington. 751 pp

Cain J. R. (2010) *Lunar dust: the hazard and astronaut exposure risks.*, Earth, Moon, Planets 107, 107–125

Cameron W. S. (1974) Manifestations and possible sources of lunar transient phenomena (LTP) (abstract). In *Lunar Interactions,* Criswell and Freeman (eds.), The Lunar Science Institute, Houston, TX, USA, p. 41.

Cameron W. S. (1978) *Lunar Transient Phenomena Catalog.*NSSDC/WDC-A-R&S 78–03, NASA Goddard Spaceflight Center, Greenbelt, Maryland.

Carrier W.D. III, Olhoeft G.R. and Mendell W. (1991) Physical properties of the lunar surface. In *Lunar Sourcebook*, Heiken G.H., Vaniman D.T. and French B.M. (eds.), Cambridge University Press, Cambridge, 475-594.

Criswell D.R. (1973) Horizon-glow and the motion of lunar dust. *In* Photon and Particle Interactions with Surfaces in Space Grard (Ed.), Reidel Publishing Co., Dordrecht, Holland, pp. 545–556.

Papike J., Ryder G. and Shearer C.K. (1998) Lunar samples. In Planetary materials, Papike J. J. (ed.) Reviews in Mineralogy and Geochemistry #36, 5-05 – 5-25.

Langevin Y. and Arnold J. R. (1977) The evolution of the lunar regolith. *Annu. Rev. Earth Planet. Sci. 5,* 449–489.

Lucey P., Korotev R. L., Gillis J. J., Taylor L. A., Lawrence D., Campbell B. A., Elphic R., Feldman B., Hood L. L., Hunten D., Mendillo M., Noble S., Papike J. J., Reedy R. C., Lawson S., Prettyman T., Gasnault O. and Maurice S. (2006) Understanding the Lunar Surface and Space-Moon Interactions. *In* New Views of the Moon, Jolliff B. L., Wieczorek M. A., Shearer C. K. and Neal C. R. (eds.) Reviews in Mineralogy and Geochemistry #60, 83–219.

McKay D. S., Fruland R. M., and Heiken G. H. (1974) Grain size and evolution of lunar soils. *Proc. Lunar Sci. Conf. 5th*,. 887–906.

McKay D. S., Heiken G., Basu A., Blanford G., Simon S., Reedy R., French B. M. and Papike J. J. (1991) The Lunar Regolith. In *LunarSourcebook*, Heiken G.H., Vaniman D.T. and French B.M. (eds.), Cambridge University Press, Cambridge, 285-356

Murphy D. L. and Vondrak R. R. (1993) Effects of levitated dust on astronomical observations from the lunar surface. Lunar and Planetary Science XXIV, 1033-1034

Noble S. K., Keller L. P. and Pieters C. M (2005) Evidence of space weathering in regolith breccias I: Lunar regolith breccias. *Meteor.& Planet. Sci.* 40, 397–408.

Olhoeft G. R., Strangway D. W., and Frisillo A. L. (1973) Lunar sample electrical properties. *Proc. Lunar Sci. Conf. 4th,* 3133–3149.

Olhoeft G. R., Frisillo A. L., Strangway D. W., and Sharpe H. (1974) Temperature dependence of electrical conductivity and lunar temperatures. *The Moon, 9,* 79–87.

Park, J.S., Y. Liu, K. D. Kihm, and L. A. Taylor (2006) Micro-Morphology And Toxicological Effects Of Lunar Dust". Lunar and Planetary Science XXXVII, asbt.# 2193.

Schwerer F. C., Huffman G. P., Fisher R. M., and Nagata T. (1974) Electrical conductivity of lunar surface rocks; laboratory measurements and implications for lunar interior temperatures. *Proc. Lunar Sci. Conf. 5th,* 2673–2687.

Stubbs T. J., Vondrak R. R. and Farrell W. M. (2006) A dynamic fountain model for lunar dust. Adv. Space Res. 37, 59–66 65

Taylor S. R. (1982) *Planetary Science: A Lunar Perspective.* Lunar and Planetary Institute, Houston, 481 pp.

Wurz P., Rohner U., Whitby J.A., Kolb C., Lammer H., Dobnikar P. and Martín-Fernández J.A., "The Lunar Exosphere: The Sputtering Contribution," Icarus 191 (2007), 486-496,